A Journal of the Gesellschaft Deutscher Chemiker

Angewandte International Edition

GDCh

Chemie

www.angewandte.org

Accepted Article

Title: Single-Layered Chiral Nanosheets with Dual Chiral Void Spaces for Highly Efficient Enantiomer Absorption

Authors: Xiaopeng Feng, Bowen Shen, Bo Sun, Jehan Kim, Xin Liu, and Myongsoo Lee

This manuscript has been accepted after peer review and appears as an Accepted Article online prior to editing, proofing, and formal publication of the final Version of Record (VoR). This work is currently citable by using the Digital Object Identifier (DOI) given below. The VoR will be published online in Early View as soon as possible and may be different to this Accepted Article as a result of editing. Readers should obtain the VoR from the journal website shown below when it is published to ensure accuracy of information. The authors are responsible for the content of this Accepted Article.

To be cited as: *Angew. Chem. Int. Ed.* 10.1002/anie.202003807

Link to VoR: https://doi.org/10.1002/anie.202003807

WILEY-VCH

10.1002/anie.202003807

WILEY-VCH

COMMUNICATION

Single-Layered Chiral Nanosheets with Dual Chiral Void Spaces for Highly Efficient Enantiomer Absorption

Xiaopeng Feng,[a] Bowen Shen,[b] Bo Sun,[a] Jehan Kim,[c] Xin Liu[a] and Myongsoo Lee*[a] [b]

[a] X. Feng, B. Sun, X. Liu, Prof. M. Lee
State Key Laboratory for Supramolecular Strucuture and Materials
College of Chemistry, Jilin University
Changchun 130012, China
[b] Dr. B. Shen, Prof. M. Lee
Department of Chemistry
Fudan University
Shanghai 200438, China
mslee@fudan.edu.cn
[c] Dr. J. Kim
Pohang Accelerator Laboratory
POSTECH
Pohang 37673, Korea

Supporting information for this article is given via a link at the end of the document.

Abstract: Although considerable effort in recent years has been devoted to the development of 2-dimensional nanostructures, single layered chiral sheet structures using lateral assembly of discrete clusters remain elusive. Here, we report single-layered chiral 2D sheet structures with dual chiral void spaces in which the discrete clusters of planar aromatic segments are arranged with in-plane AB order in aqueous methanol solution. The chirality of the sheet is induced by the slipped-cofacial stacks of rectangular plate-like aromatic segments in the discrete clusters which are arranged laterally with up the down packing, resulting in dual chiral void spaces. The chiral nanosheets function as superfast enantiomer separation nanomaterials which absorb rapidly a single enantiomer in a racemic mixture with greater than 99 %*ee*.

Construction of two-dimensional (2-D) nanostructures is an attractive target owing to their unique properties for many promising applications in separation, energy storages, optoelectronics, and catalysis.[1-4] However, it remains a challenge to synthesize single-layered 2D sheet structures without using 2D templates, which are essential for unique structural, mechanical, and electronic properties that make them highly attractive in many applications.[5-9] The single-layered sheets can be constructed by the self-assembly of multipod aromatic segments[10-12] or macrocycle amphiphiles,[13] and the exfoliation of metal-organic or covalent organic frameworks.[14-16] Despite such recent achievements in 2-D materials, most of the 2D framework structures are far from the optically active properties for chiral recognition since such framework design encounters difficulties of breaking mirror symmetry in 2-dimension. The twisted stacks in one direction of flat objects overcome this problem due to mirror symmetry breaking, as exemplified in a twist stacking of bilayer graphene.[17] The symmetry breaking by twisting can be applied to macrocycle stacks to generate chiral pores.[18] For example, faced macrocycle dimers by twisting with respect to each other in one direction induce pore chirality by breaking mirror symmetry.[19] The twisted dimeric stacks with chiral interior laterally associate to form single-layered chiral sheet structures, while prohibiting layer stacks because the 2-D aromatic surfaces are covered by the flexible chains. Another approach to 2D chiral structures is provided by lateral assembly of helical nanofibers which provide chiral void spaces.

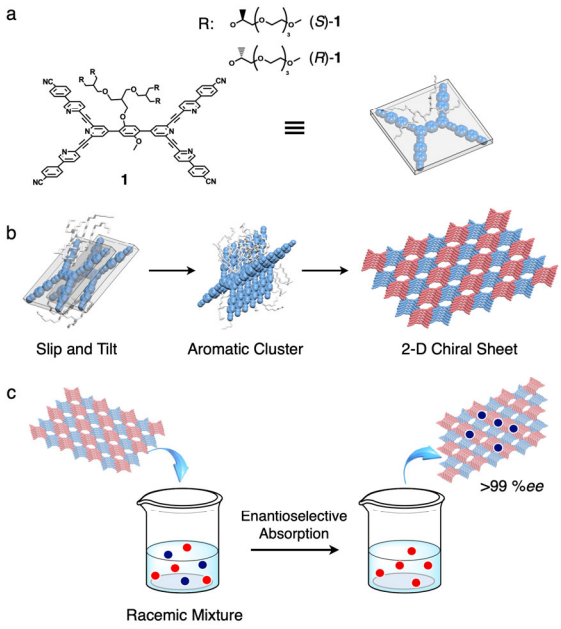

Figure 1. (a) Molecular structure of **1*S***. (b) Schematic representation for the formation of a single-layered chiral nanosheet structure through lateral assembly of chiral clusters consisting of slipped planar aromatic segments. (c) Enantioselective absorption of the chiral sheets in a racemic mixture solution.

For example, laterally grafted rod-like α-helical peptides can be aligned parallel to each other to self-assemble into 2-D chiral sheet structures.[20] Considering the parallel arrangements of the helical peptides, the void spaces formed between the helical peptide arrangements are chiral, which discriminate one enantiomer from

This article is protected by copyright. All rights reserved.

Accepted Manuscript

10.1002/anie.202003807

racemic mixture solution. Despite such notable examples of 2-D chiral materials, single-layered chiral sheets with dual chiral domains remain elusive. Here, we report single-layered chiral 2-D sheet structures with dual chiral void spaces formed by in-plane AB order Of chiral clusters in aqueous methanol solution (Figure 1). The chirality of the sheets is induced by a slipped-cofacial stack of rectangular-shaped coplanar aromatic segments with a preferred direction in clusters that are arranged laterally with up and down in-plane packing, resulting in dual chiral void spaces. Notably, the single-layered nanosheets with chiral void spaces function as highly efficient enantiomer absorbing nanomaterials which absorb rapidly one enantiomer in a racemic mixture solution with greater than 99 %*ee*.

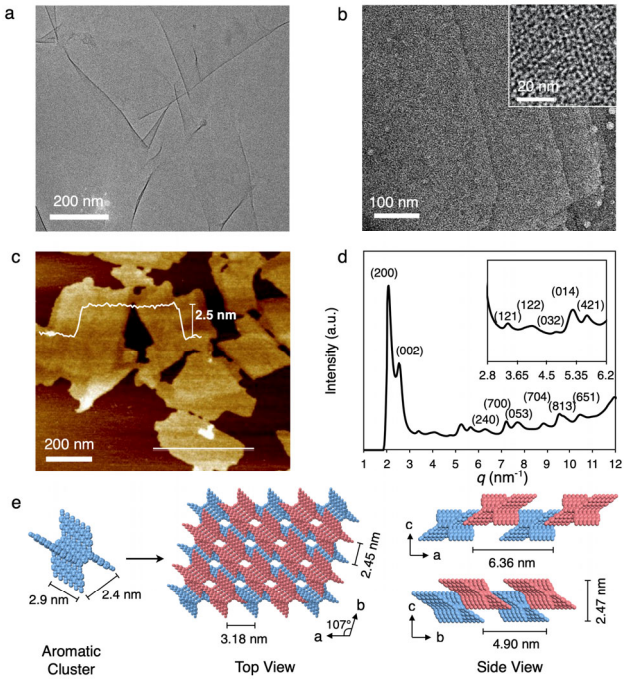

Figure 2. (a) Cryo-TEM image of **1*S*** (138 μM) in aqueous methanol solution (3/7, v/v). (b) Negatively-stained TEM image from the cast film of **1*S***, inset: high resolution TEM image of **1*S***. (c) AFM height image of the sheets on mica surface from evaporation of **1*S*** (46 μM) in aqueous methanol solution (3/7, v/v). The cross-sectional profile (top) is taken along the white line. (d) SAXS pattern of ***1S*** with a freeze-dried sample. (e) Schematic illustration of the sheet formed from lateral assembly of a cluster showing the top view (middle) and side views (right).

We envisioned that, when a rectangular plate-like aromatic building block is face-on grafted by a chiral flexible chain, the aromatic stack would be associated with slipping in a preferred direction caused by chiral transfer to break mirror symmetry, resulting in a chiral superstructure (Figure 1b).[21-23] In this context, we synthesized a rectangular-shaped, planar aromatic segment with a hydrophilic chiral dendron at the center of the basal plane. The amphiphilic molecule (**1**) that forms a 2-D porous structure consists of a tetrabranched aromatic segment and an internally-grafted oligoether dendron. The amphiphilic molecule was synthesized from commercially available starting materials in a stepwise manner according to the procedures described in Supporting Information. The resulting amphiphilic molecule was characterized by ^{1}H- and ^{13}C-NMR spectroscopies, and MALDI-TOF mass spectroscopy which were shown to be in full agreement with the chemical structure presented (Figure S1 and S2).

To investigate aggregation behavior in bulk solution, we performed cryogenic transmission electron microscopy (cryo-TEM) using a freeze aqueous methanol solution (3/7, v/v) of **1**. The image showed flat 2D sheet objects with straight edges, ranging in their lateral dimensions from sub-micrometer to several micrometers (Figure 2a), indicating that **1** self-assembles into a 2-D flat sheet structure in bulk solution. To obtain more structural information on the sheets, TEM experiments were performed with negatively stained films. The image revealed flat 2-D sheet structures with straight edges (Figure 2b), consistent with the cryo-TEM result. A high-resolution image revealed 2-D organized aromatic domains with an oblique lattice (Figures 2b, inset). Selected area electron diffraction (SAED) showed a light spot pattern in a dark background corresponding to an oblique lattice with in-plane dimensions of a = 3.18 nm and b = 2.45 nm, and a characteristic angle of 107° (Figure S7). Atomic force microscopy (AFM) analysis showed that the nanosheets are very flat with a uniform thickness of 2.5 nm (Figure 2c).

To gain more insight into the 2-D nanosheet structure, X-ray experiments were performed with freeze-dried samples of **1**. Small-angle X-ray scatterings (SAXS) showed a number of sharp reflections which agree well with the expected relative peak positions for a 3-D monoclinic structure with lattice parameters of a = 6.36 nm, b = 4.90, c = 5.04 nm, and γ = 107° (Figure 2d and Table S1). Considering the layer thickness of 2.5 nm determined from AFM, this result indicates that the single layered porous nanosheets are stacked in an ABAB fashion. It is notable that the in-plane lattice constants a and b are twice larger than those determined from SAED, thus the in-plane SAED spots can be indexed as (200) and (020) reflections. These results indicate that the aromatic domains are laterally arranged in ABAB order to form a single-layered 2-D sheet structure (Figure 2e). The wide-angle X-ray diffraction pattern shows a sharp reflection associated with a π-π stacking distance of 0.38 nm (Figure S8), indicative of the close packing of the plate-like aromatic segments in the aromatic domains.

Considering the lattice parameters and the measured density of 1.17 g/ml, the number of molecules consisting of a primary structure can be calculated to be 6 (Table S2). When compared with the molecular length in the diagonal aromatic axis of **1**, the layer thickness of 2.5 nm indicates that the molecules are tilted with an angle of ~52° with respect to the c-axis (Figure S8). Consequently, the tilted packing of 6 molecules gives rise to a discrete aromatic cluster with in-plane dimensions of 2.9 nm and 2.4 nm as a discrete primary structure of the 2D sheet assembly (Figure 2e and S8). To further corroborate the primary structure of the sheets, TEM experiments were

This article is protected by copyright. All rights reserved.

Accepted Manuscript

10.1002/anie.202003807

performed with highly-diluted solution of **1**. When diluted, TEM showed the formation of well-separated discrete nanostructures which, subsequently, self-assemble laterally into 2-D planar structures at higher concentrations (Figure S9), indicating that the primary structure of the 2-D sheets is a discrete aromatic cluster. This result demonstrates that the discrete clusters formed in earlier stages of the self-assembly propagate in 2-dimensions to form a single-layered sheet with increasing concentration (Figure 3).
The formation of the discrete clusters with tilting of the aromatic segments in a 2-D sheet arises from the tendency of rectangular plate-like aromatic blocks to form aromatic π-stacks and consequent space-filling requirements.[24]

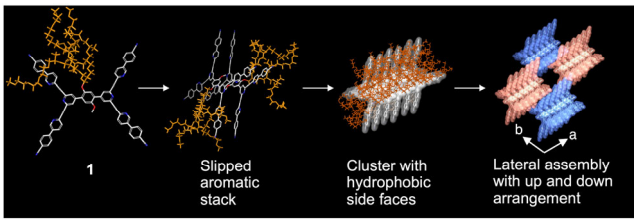

Figure 3. Schematic illustration of the self-assembly of **1** into discrete clusters consisting of 6 molecules with slipped packing. The clusters with hydrophobic side faces laterally associate through side-by-side hydrophobic interactions to generate a 2-D sheet structure in aqueous methanol solution.

The molecular architecture comprising a planar aromatic segment and a flexible dendrimer segment drives a nanophase separation due to large chemical differences between each segment. However, fully-overlapped stacking of the plate-like aromatic parts would confine grafting junctions to a flat and continuous interface with a high density of grafting sites, resulting in strong space crowding with chain deformation. To minimize chain deformation and fill space efficiently, the fully-overlapped aromatic stacking would be broken into discrete nanostructures with slipped packings by splaying the flexible chains to provide larger interfacial area, giving rise to a chiral aromatic cluster. Indeed, when circular dichroism (CD) spectroscopy experiments were applied to the sheet structures, the sheet solution of **1*S*** revealed a strong negative Cotton effect (Figure 4a), demonstrating that the slipped cofacial stack of planar aromatic segments generates a chiral superstructure.[25] The sheet solution of **1*R*** formed from the enantiomer exhibits opposite CD signal with a perfect mirror image relationship, indicating that the chirality of the dendrimer chain is communicated with the aromatic packings to form chiral 2-D sheet structures.
Taken all data together, we propose that the slipped cofacial stacks of rectangular plate-like aromatic segments generate chiral aromatic clusters with hydrophobic side faces. Consequently, the chiral clusters hierarchically assemble through side-by-side hydrophobic interactions to form a single layered structure, simultaneously prohibiting 3-D layer stacking in aqueous methanol solution due to the hydrophilic dendrimer chains located at a c-direction of the cluster surface. Considering the shape of the cluster with protruded aromatic side parts and the lattice parameters, 2-dimensional arrangements of the clusters can be illustrated by in-plane up and down ABAB order, as reflected in the SAXS pattern (Figure 2d). Taking into account that the 2D sheets of **1** consist of slipped aromatic chiral clusters with in-plane up and down AB packing, the in-plane hydrophilic dendrimer domains formed between the clusters would be alternatively-arranged two different chiral spaces (Figure 4b).[21] Accordingly, we envisioned that the hydrophilic domains in an aromatic matrix can play as a role in chiral containers for entrapping hydrophobic guests in a hydrophilic solvent, so that the 2D sheet with ordered chiral hydrophilic domains functions as enantioselective absorbing 2D materials as the one enantiomer over the other one preferentially bind to chiral void spaces.[26,27]
To explore the capability of the self-assembled sheets for enantioselective absorption, hydrophobically substituted tartrate (**G1**) was selected because the void space consists of hydrophobic, aromatic interior walls, of which the in-plane size is roughly compatible with the guest size with a folded conformation (Figure S8 and S11). To corroborate chiral discrimination, we added a racemic tartrate derivative (17 μM) to a solution (46 μM) of **1*S***. The internalization of the guest within the void space interior was confirmed by tracing high-performance liquid chromatography (HPLC) after separation of the untrapped racemate from the sheet solution by gel permeation chromatography (GPC) using a Sephadex LH-20 column. After saturated adsorption with briefly shaking for several minutes, we found that the void spaces of ~47% uptake the tartrate guest (Figure 4c and S12). This uptake result is not unexpected because the in-plane up and down arrangements of the tilted aromatic clusters generate two different chiral void spaces with non-mirror images of one another (Figure 4b). As a result, **G1** fits well into only one of the two different chiral void spaces, while does not compatible with the other void. This was further confirmed by titration experiments using a pure **G1** enantiomer that showed 50% uptake of the pores (Figure S13 and S14).
The preferential capture of the enantiomers after saturated absorption for several minutes was then monitored by tracing chiral HPLC. The profile showed that the peak associated with the L-enantiomer of the tartrate guest appears without any noticeable trace associated the D-enantiomer (Figure 4d), demonstrating that the porous sheets of **1*S*** exclusively uptake the L-form with perfect inclusion preference over the D-form (>99% *ee*). Consistent with the HPLC separation result, NMR experiments showed the resonance peaks associated with the aromatic protons of the guest are upfield shifted at the range of 7.4-7.8 ppm in the sheet solution (Figure 4e), indicating that the chiral guest is entrapped in the void spaces of the sheet through host-guest aromatic interactions.[28] This aromatic coupling was further confirmed by fluorescence quenching at 450 nm on entrapping the guests (Figure 4f). In sharp contrast, the nanosheet of **1*S*** does not exhibit apparent inclusion activity for the D-enantiomer (Figure S15), demonstrating that the enantiomer is not

This article is protected by copyright. All rights reserved.

Accepted Manuscript

10.1002/anie.202003807

fit into the void spaces of **1*S***. On the contrary, **1*R*** sheets uptake exclusively D-form in the racemic tartrate solution, demonstrating that the enantioselective absorption of the sheets in a racemic mixture solution arises from the chirality of the sheet (Figure 4d). To evaluate enantioselectivity of the sheets with different guests, we carried out the same experiments of **1*S*** with hydrophobically-substituted phenylalanine (**G2**).

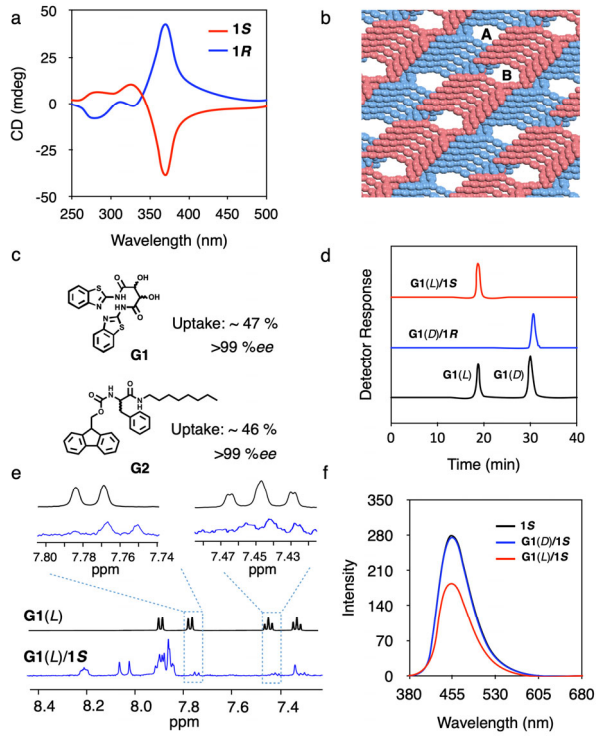

Figure 4. (a) CD spectra of **1*S*** (red) and **1*R*** (blue) (46 μM) aqueous methanol solution (3/7, v/v). (b) Schematic illustration of the sheet consisting of alternatively-arranged A and B hydrophilic domains. (c) Molecular structure of guests **G1** and **G2**. (d) Chiral-HPLC traces of a racemic **G1**(black), selective uptake of the L form by **1*S*** (red), and selective uptake of the D form by **1*R*** (blue) in aqueous methanol solution (3/7, v/v). (e) ^{1}H-NMR spectra of **G1**(*L*) (42 μM) with **1*S*** (460 μM) (blue) and without **1*S*** (black) in methanol-*d4*/THF-*d8* solution (9/1, v/v). (f) Fluorescence spectra from **1*S*** (46 μM) aqueous methanol solution (3/7, v/v) with **G1**(*L*) (4.2 μM) (red), **G1**(*D*) (4.2 μM) (blue) and without guest (black).

Similar to the tartrate derivative, the chiral sheet showed 46 % uptake of the void spaces for **G2** and the enantioselectivity to be nearly perfect (>99% *ee*) (Figure S12 and S17). The clear-cut enantioselectivity with very fast absorption in a racemic guest solution indicates that the lateral arrangement of the chiral clusters into a single layer generates 2-dimensional chiral void spaces, enabling the sheets to absorb only a preferred enantiomer in a racemic mixture solution with only one discrimination event, either binding or non-binding (Figure 1c).[29] As a result, our approach can allow for the construction of superfast separation materials with perfect enantiomer selectivity. This is in great contrast to current enantio-separation materials which rely on a series of interactions between a racemic mixture and pore walls.[30-32]

In conclusion, we have constructed single-layered chiral sheet structures in aqueous MeOH solution using self-assembly of a rectangular plate-shaped aromatic amphiphile. The 2-D chiral sheets consist of lateral arrangement of chiral aromatic clusters with in-plane up and down AB order, generating dual chiral void spaces in a hydrophilic solvent. The nanosheets with chiral void spaces function as superfast enantiomer separation nanomaterials which absorb rapidly a single enantiomer in a racemic mixture with enantiomeric excess (*ee*) greater than 99 %. We anticipate that our strategy to construct 2-D chiral materials will provides access to porous 2-dimensional materials with complex functions capable of performing multiple separations and multiple chemical reactions.

Acknowledgements

This work was supported by the National Natural Science Foundation of China (21634005 and 51473062) and Fudan Research Fund.

Keywords: supramolecular assembly • chiral nanosheet • dual chiral domains • enantiomer absorption

[1] F. Shahzad, M. Alhabeb, C. B. Hatter, B. Anasori, S. Man Hong, C. M. Koo, Y. Gogotsi, *Science* **2016**, *353*, 1137-1140.

[2] D. Sheberla, L. Sun, M. A. Blood-Forsythe, S. Er, C. R. Wade, C. K. Brozek, A. Aspuru-Guzik, M. Dincă, *J. Am. Chem. Soc.* **2014**, *136*, 8859-8862.

[3] E. Jin, M. Asada, Q. Xu, S. Dalapati, M. A. Addicoat, M. A. Brady, H. Xu, T. Nakamura, T. Heine, Q. Chen, D. Jiang, *Science* **2017**, *357*, 673-676.

[4] S. Yuan, X. Li, J. Zhu, G. Zhang, P. Van Puyvelde, B. Van der Bruggen, *Chem. Soc. Rev.* **2019**, *48*, 2665-2681.

[5] a) L. Lafferentz, V. Eberhardt, C. Dri, C. Africh, G. Comelli, F. Esch, S. Hecht, L. Grill, *Nat. Chem.* **2012**, *4*, 215-220; b) K. Baek, I. Hwang, I. Roy, D. Shetty, K. Kim *Acc. Chem. Res.* **2015**, *48*, 2221-2229; c) S.-Q. Xu, X. Zhang, C.-Bi.Nie, Z.-F. Pang, X.-N. Xua, Xin Zhao *Chem. Commun.* **2015**, *51*, 16417-16420; d) S. Shin, S. Lim, Y. Kim, T. Kim, T.-L. Choi, M. Lee *J. Am. Chem. Soc.* **2013**, *135*, 2156-2159; e) K. T. Nam, S. A. Shelby, P. H. Choi, A. B. Marciel, R. Chen, L. Tan, T. K. Chu, R. A. Mesch, B.-C. Lee, M. D. Connolly, C. Kisielowski, R. N. Zuckermann *Nat. Mater.* **2010**, *9*, 454-460; f) Y. Wang, Y. Kim, M. Lee *Angew. Chem. Int. Ed.* **2016**, *55*, 13122–13126; *Angew. Chem. Int. Ed.* **2016**, *10*, 13316-13320; g) S. Ghosh, D. S. Philips, A. Saeki, A. Ajayaghosh *Adv. Mater.* **2017**, *29*, 1605408.

[6] X. Gao, Y. Zhu, D. Yi, J. Zhou, S. Zhang, C. Yin, F. Ding, S. Zhang, X. Yi, J. Wang, L. Tong, Y. Han, Z. Liu, J. Zhang, *Science Adv.* **2018**, *4*, eaat6378.

[7] P. Payamyar, B. T. King, H. C. Öttinger, A. D. Schlüter, *Chem. Commun.* **2016**, *52*, 18-34.

[8] J. W. Colson, A. R. Woll, A. Mukherjee, M. P. Levendorf, E. L. Spitler, V. B. Shields, M. G. Spencer, J. Park, W. R. Dichtel, *Science* **2011**, *332*, 228-231.

[9] R. Dong, M. Pfeffermann, H. Liang, Z. Zheng, X. Zhu, J. Zhang, X. Feng, *Angew. Chem.* **2015**, *127*, 12226-12231; *Angew. Chem. Int. Ed.* **2015**, *54*, 12058-12063.

[10] K.-D. Zhang, J. Tian, D. Hanifi, Y. Zhang, A. C.-H. Sue, T.-Y. Zhou, L. Zhang, X. Zhao, Y. Liu, Z.-T. Li, *J. Am. Chem. Soc.* **2013**, *135*, 17913-17918.

[11] L. Yue, S. Wang, D. Zhou, H. Zhang, B. Li, L. Wu, *Nat. Commun.* **2016**, *7*, 10742.

[12] K. Baek, I. Hwang, I. Roy, D. Shetty, K. Kim, *Acc. Chem. Res.* **2015**, *48*, 2221-2229.

[13] Y. Kim, S. Shin, T. Kim, D. Lee, C. Seok, M. Lee, *Angew. Chem.* **2013**, *125*, 6554-6557; *Angew. Chem. Int. Ed.* **2013**, *52*, 6426-6429.

[14] Y. Peng, Y. Li, Y. Ban, H. Jin, W. Jiao, X. Liu, W. Yang, *Science* **2014**, *346*, 1356-1359.

This article is protected by copyright. All rights reserved.

Accepted Manuscript

[15] S.-L. Cai, W.-G. Zhang, R. N. Zuckermann, Z.-T. Li, X. Zhao, Y. Liu, *Adv. Mater.* **2015**, *27*, 5762-5770.
[14] P. Kissel, D. J. Murray, W. J. Wulftange, V. J. Catalano, B. T. King, *Nat. Chem.* **2014**, *6*, 774-778.
[17] C.-J. Kim, A. Sánchez-Castillo, Z. Ziegler, Y. Ogawa, C. Noguez, J. Park, *Nat. Nanotech.* **2016**, *11*, 520-524.
[18] B. Shen, Y. Kim, M. Lee, *Adv. Mater.,* DOI:10.1002/adma.201905669
[19] B. Sun, Y. Kim, Y. Wang, H. Wang, J. Kim, X. Liu, M. Lee, *Nat. Mater.* **2018**, *17*, 599-604.
[20] a) X. Chen, Y. Wang, H. Wang, Y. Kim, M. Lee, *Chem. Commun.* **2017**, *53*, 10958-10961; b) X. Chen, Y. He, Y. Kim, M. Lee, *J. Am. Chem. Soc.* **2016**, *138*, 5773-5776.
[21] M. Miyata, N. Tohnai, I. Hisaki, T. Sasaki, *Symmetry* **2015**, *7*, 1914-1928.
[22] T. Kajitani, K. Motokawa, A. Kosaka, Y. Shoji, R. Haruki, D. Hashizume, T. Hikima, M. Takata, K. Yazawa, K. Morishima, M. Shibayama, T. Fukushima, *Nat. Mater.* **2019**, *18*, 266-272.
[23] Y. Wang, J. Xu, Y. Wang, H. Chen, *Chem. Soc. Rev.* **2013**, *42*, 2930-2962.
[24] M. Lee, B.-K. Cho, Y.-G. Jang, W.-C. Zin, *J. Am. Chem. Soc.* **2000**, *122*, 7449-7455.
[25] a) A. Raudino, M. Pannuzzo, The *J. Chem. Phys.* **2012**, *137*, 134902; b) Y. Kim, J. Kang, B. Shen, Y. Wang, Y. He, M. Lee, *Nat. Commun.* **2015**, *6*, 8650; c) M. Morisue, H. Fukui, M. Shimizu, K. Inoshita, Y. Morisaki, Y. Chujo, *Tetrahedron Letters* **2014**, *55*, 271-274.
[26] L. Chen, P. S. Reiss, S. Y. Chong, D. Holden, K. E. Jelfs, T. Hasell, M. A. Little, A. Kewley, M. E. Briggs, A. Stephenson, K. M. Thomas, J. A. Armstrong, J. Bell, J. Busto, R. Noel, J. Liu, D. M. Strachan, P. K. Thallapally, A. I. Cooper, *Nat. Mater.* **2014**, *13*, 954-960.
[27] Y. Peng, T. Gong, K. Zhang, X. Lin, Y. Liu, J. Jiang, Y. Cui, *Nat. Commun.* **2014**, *5*, 4406.
[28] a) J. S. Mugridge, R. G. Bergman, K. N. Raymond, *J. Am. Chem. Soc.* **2011**, *133*, 11205-11212; b) A. S. Shetty, J. Zhang, J. S. Moore, *J. Am. Chem. Soc.* **1996**, *118*, 1019-1027.
[29] A. W. Hauser, N. Mardirossian, J. A. Panetier, M. Head-Gordon, A. T. Bell, P. Schwerdtfeger, *Angew. Chem.* **2014**, *126*, 10117-10120; *Angew. Chem. Int. Ed.* **2014**, *53*, 9957-9960.
[30] R. Xie, L.-Y. Chu, J.-G. Deng, *Chem. Soc. Rev.* **2008**, *37*, 1243-1263.
[31] M. N. Corella-Ochoa, J. B. Tapia, H. N. Rubin, V. Lillo, J. González-Cobos, J. L. Núñez-Rico, S. R. G. Balestra, N. Almora-Barrios, M. Lledós, A. Güell-Bara, J. Cabezas-Giménez, E. C. Escudero-Adán, A. Vidal-Ferran, S. Calero, M. Reynolds, C. Martí-Gastaldo, J. R. Galán-Mascarós, *J. Am. Chem. Soc.* **2019**, *141*, 14306-14316.
[32] X. Han, J. Huang, C. Yuan, Y. Liu, Y. Cui, *J. Am. Chem. Soc.* **2018**, *140*, 892-895.

WILEY-VCH

Accepted Manuscript

This article is protected by copyright. All rights reserved.

10.1002/anie.202003807

WILEY-VCH

COMMUNICATION

Entry for the Table of Contents

Insert graphic for Table of Contents here.

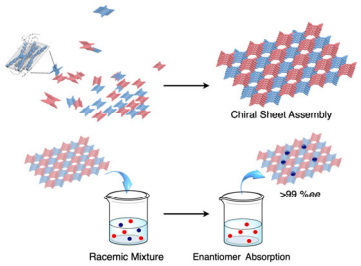

Single-layered chiral 2D sheet structures with dual chiral void spaces are formed from the discrete clusters with in-plane up and down AB packing in aqueous methanol solution. The slipped-cofacial stacks of rectangular plate-like aromatic segement induce the chirality of sheet. The nanosheets absorb rapidly one enantiomer from racemic mixture solution with enantiomeric excess (*ee*) of greater than 99 %.

WILEY-VCH

Accepted Manuscript

This article is protected by copyright. All rights reserved.